PAGEOPH, Vol. 146, No. 2 (1996) 0033-4553/96/020343-21$1.50 + 0.20/0

A Direct Method of Calculating Interval Velocities and Layer Thicknesses from Wide-angle Seismic Reflection Times

KALACHAND SAIN[1] and K. L. KAILA[2]

Abstract—Wide-angle reflections are now routinely recorded in high resolution explosion seismics to study the crustal structure. Use of Dix's hyperbolic approximation to the nonhyperbolic wide-angle reflection travel times causes major errors in the determination of interval velocities and layer thicknesses of a stack of horizontal velocity layers. Here we propose a layer stripping method to directly calculate the interval velocities and layer thicknesses in a vertically heterogeneous earth from the strong and reliable wide-angle reflected events. Synthetic reflection travel times, at wide-angle range, for a given velocity model, contaminated by some random errors, have been used to demonstrate the reliability of the algorithms to determine the interval velocities and thicknesses of various layers. The method has also been tested on two field examples along two deep seismic sounding (DSS) profiles with well identified wide-angle reflection travel times, which illustrates the practical feasibility of the proposed method.

Key words: Wide-angle reflection times, interval velocities and thicknesses, stripping method.

Introduction

Recording of wide-angle seismic waves generated from controlled sources has become a very important tool to obtain deeper crustal information about velocity and regional structure in any area. Because of the sudden increase in the reflection coefficient near the critical angle (RICHARDS, 1961; WINTERSTEIN and HANTEN, 1985), the amplitudes of post critical (wide-angle) reflection events are very large due to total internal reflection. Wide-angle events from intra- and subcrustal horizons associated with a small velocity jump (less than 0.4 km/s) stand out clearly on the seismogram even in a noisy area. Many excellent examples of the same are available in a review of such studies in central Europe, edited by GIESE *et al.* (1976).

Interpretation of wide-angle reflection travel times is beset with several difficulties such as lateral inhomogeneities, block structures, steeply dipping events, etc. Even if the simplifying assumption of lateral homogeneity is made, the

[1] National Geophysical Research Institute, Hyderabad-500007, India.
[2] 2-16-106, Prashantinagar, Uppal Road, Hyderabad-500039, India.

refraction effects at each overlying interface of a stack of horizontal velocity layers increase with increasing offset and become very large at the wide-angle range. The reflection travel times at large offset are explained by nonhyperbolic series (TANER and KOEHLER, 1969). However, to date, hyperbolic approximation (neglecting the third and higher order terms of the series) which is valid only at small offset, is used for seismic data processing. KAILA an SAIN (1994) show that percentage errors in rms velocity and zero offset two-way travel time increase manifold as determined from wide-angle reflection times by hyperbolic approximation without any control at low angle region. On the other hand, these errors are reduced considerably with successive inclusion of higher order terms of the series. They mention that more than two coefficients polynomial fit needs data accuracy up to a fraction of a millisecond which is, at present, not attainable with real data sets. AL-CHALABI (1974) pointed out that velocity determination from large offset reflection times by hyperbolic approximation causes errors in the determination of interval velocities unless an appropriate adjustment is allowed for refraction effects. Al-Chalabi's method of extrapolation back to the zero effective offset is a good approach to estimate the rms velocity from stacking velocities. However, when the same principle is applied to wide-angle reflection travel times, though the method reduces the error in rms velocity, the overall errors are still too substantial to be ignored unless one uses constraints from the low-angle range. KAILA and KRISHNA (1979) evaluated effective velocity from reversed reflection travel times at large offsets or wide-angle range, considering all overlying layers as an effective single layer to calculate the depth to the interface but the interval velocity analysis has remained rather difficult.

Different authors have determined interval velocities and layer thicknesses from large offset reflection times in different ways. DIX's (1955) interval velocity formula can be used only when rms velocities and two-way travel times close to zero offset are known. As the offset increases, the estimated velocity, called slant path rms velocity (ROBINSON, 1983), obtained by hyperbolic fitting, is different from Dix's rms velocity due to refraction of the ray at each overlying interface. Unless the refraction effects are taken into account, the velocity analysis will be erroneous and this error will be massive at the wide-angle range. To consider the refraction effects, SATTLEGGER (1965) proposed an iterative method which considers the exact ray path in a multilayered earth in the computation of travel times for a given velocity model. These travel times are then compared with the observed travel times by a least-squares method, based on Gauss-Newton solution. This method is applicable only to some limited offset travel times for which refraction effects are very small. LIMOND and PATRIAT (1975) made use of Sattlegger's method in the computation of forward response to match the wide-angle reflections in marine sonobuoy work by a least squares method in which only velocity is varied while constraining the zero offset travel time from a normal incidence reflection profile. Without using any constraints from normal incidence reflection profiles, SAIN and KAILA (1994) proposed an iterative method of computing interval velocities and layer thicknesses from a set of wide-angle reflection travel times, using a damped least-squares technique. Here we propose a method to directly calculate the interval velocity and thickness of a layer from wide-angle seismic reflection travel times by a layer stripping method, keeping parameters (once estimated) of all overlying layers fixed.

To calculate interval velocities from reflection travel times at any offset, GARMANY *et al.* (1979), DIEBOLD and STOFFA (1981), and SCHULTZ (1982) presented techniques which need transformation of the $X - T$ data to the $\tau - p$ domain, where p $(=dT/dX)$ is the ray parameter and τ equals to $T - pX$. The τ, T and X are the intercept time, the two-way travel time and the offset distance, respectively. In our proposed method, we show that even without transforming the coordinates in the $\tau - p$ domain, the layer parameters can be calculated quite accurately from any set of wide-angle reflection times. NOWROOZI's (1990) direct method of calculating interval velocities and layer thicknesses, of course, needs no transformation of data but his method requires recognition of the (X, T) pairs of reflected phases from the top and the bottom of a layer, associated with the same ray parameter, to calculate the interval velocity and thickness of that layer. For field data which contain many errors, at a particular wide-angle recording spread, recognition of the same ray parameter from the top and the bottom of a layer can be rather very difficult. The same ray parameter from the top and the bottom of the layer may not be available at a given recording spread and hence direct calculation of interval velocity and layer thickness from wide-angle reflection phases by Nowroozi's method is not always promising. On the other hand, we can calculate, by a new approach discussed in this paper, the ray parameters at points of observation lying at any wide-angle recording offset, which can be used to strip off the contributions to the offsets and travel times of all overlying layers.

Laterally homogeneous velocity structure is assumed in all 1-*D* forward modeling of travel times and amplitudes (FUCHS and MUELLER, 1971), Wiechert-Herglotz inversion (BULLEN and BOLT, 1985) and $\tau - p$ inversion (DIEBOLD and STOFFA, 1981). The advantage of 1-*D* modeling is that they are relatively quick and easy to implement as compared to 2-*D* techniques which need very good starting models. Our direct method of calcuating interval velocities and thicknesses of various layers from unreversed reflection times serves as a good starting model for the 2-*D* modeling.

Synthetic reflection times at wide-angle range, contaminated by some random errors, for a given velocity model, have been used to calculate the layer parameters by the proposed method. The study presents a very good estimation of the layer parameters with small mean errors for a number of models. This serves as a good indicator of the reliability of the proposed method for velocity analysis from wide-angle reflection times. Application of the method on well identified field examples demonstrates the practical feasibility of the method.

Theory of the Proposed Method: Velocity Analysis

Velocity analysis, i.e., calculation of interval velocities and layer thicknesses of a stack of horizontal velocity layers, is often done fitting reflection times by Dix's hyperbolic equation. To investigate the deep continental crust, wide-angle reflections are being extensively used in the USSR, USA, Canada, parts of Europe and India. Marine seismic experiments using long towed arrays or multiple ship operations acquire seismic data with large source-receiver offsets (STOFFA and BUHL, 1980; STOFFA *et al.*, 1981, 1982). The velocity-depth information derived using Dix's formula degrades when hyperbolic approximation is used to fit the $(X-T)$ data at large offsets (CRESSMAN, 1968; BROWN, 1969; TANER and KOEHLER, 1969; TANER *et al.*, 1970). Corrections for it are approximate, model dependent or require iterative application (SATTLEGGER, 1965; AL-CHALABI, 1974; HUBRAL and KREY, 1980).

Velocity-depth information in the $\tau - p$ domain improves in contrast to the hyperbolic travel time approximation as additional ray parameters are observed. The $\tau - p$ inversion (DIEBOLD and STOFFA, 1981), layer stripping method (SCHULTZ, 1982), an approximate method based on finding the best single ellipse (CUTLER and LOVE, 1980), are very well known methods in the $\tau - p$ domain. When only discrete $X - T$ data at wide-angle range over a recording length of say 20 to 30 km, are available, calculation of the ray parameter at each observational point by the standard slope-intercept method becomes problematic. Again, if limited values of ray parameters and intercept times are available, fitting by elliptical equation also produces large errors in the calculation of interval velocities and layer thicknesses. For field data which contain many errors, ray parameters, calculated at various observational points by drawing the tangent to the $X - T$ data, do not always show the increasing trend of the ray parameters with offset. BESSONOVA *et al.* (1974) calculated $\tau(p)$ from a set of discrete travel-time data (T_i, X_i), based on the extremum property of $T(p_0) - pX(p_0)$ as p_0 is varied with p fixed. $T_i - pX_i$ is plotted for a fixed value of p as a function of X_i. The extreme value of $T_i - pX_i$ is euqal to $\tau(p)$ at $X(p)$ and hence p is known at same X. Another fixed value of p which differs very little from the earlier one gives the extreme value of $T_i - pX_i$ at another point of $X(p)$. For many data points, this method needs one such search for each data point (T_i, X_i) through a careful selection of p. Our method of calculating p is very simple and reliable even from noisy wide-angle seismic data and we need not form a chart to calculate the ray parameters at various points of a set of discrete data. Of course, the error in calculating p is proportional to that in the observed travel-time data. The knowledge of ray parameters enables one to calculate for any (X, T)-point of a reflection travel-time data set the contributions to the travel times and offset distances due to overlying layers. After subtracting these contributions we derive travel times and offsets associated with the layer from the bottom of which the reflections are under

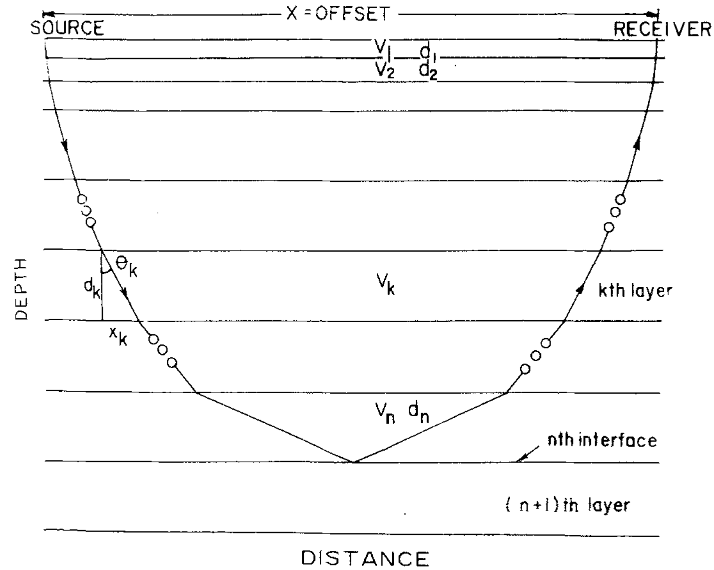

Figure 1
Reflection ray path in homogeneous, isotropic and horizontal layers with various parameters defined.

consideration. These times and offsets are related by the hyperbolic equation perfectly and therefore directly yield accurate values of the interval velocity and the thickness of the layer concerned.

For a medium consisting of n homogeneous, isotropic and horizontal layers, the reflection time $T(X)$ and offset X are expressed as a function of layer parameters (velocities and thicknesses) and ray parameter p as,

$$T(X) = 2 \sum_{k=1}^{n} d_k/[v_k(1 - p^2 v_k^2)^{1/2}], \tag{1}$$

$$X = 2p \sum_{k=1}^{n} d_k v_k/(1 - p^2 v_k^2)^{1/2}, \tag{2}$$

where p is defined by Snells law as,

$$p = \sin(\theta_k)/v_k, \tag{3}$$

θ_k is the angle of down-going or upcoming ray at the kth layer with respect to the vertical. θ_k, x_k, v_k, d_k, and X are defined in Figure 1. For the case of a single layer,

$$T(X) = 2d_1/[v_1(1 - p^2 v_1^2)^{1/2}], \tag{4}$$

$$X = 2pd_1 v_1/[1 - p^2 v_1^2]^{1/2}. \tag{5}$$

Equations (4) and (5) are related as

$$T^2(X) = X^2/v_1^2 + 4\, d_1^2/v_1^2, \tag{6}$$

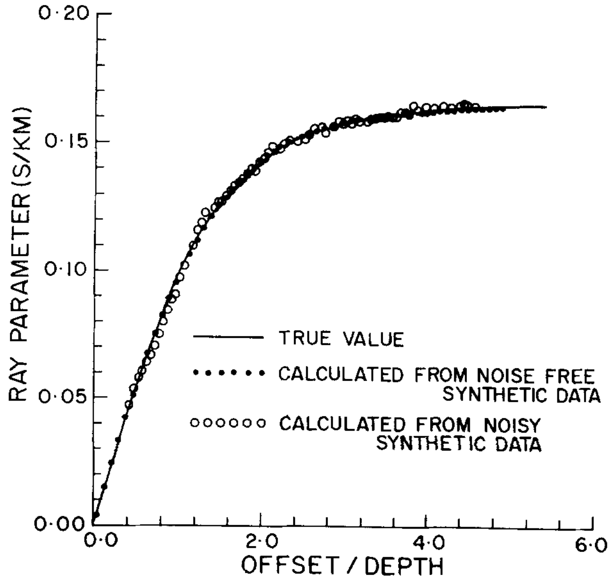

Figure 2
Comparison between true ray parameters and those calculated by the proposed method from noisy and noise-free synthetic reflection travel times corresponding to the bottom layer of the model shown in Figure 3. Ray parameter at midpoint of each segment is compared.

which is purely hyperbolic, and by a simple $T^2(X)$ versus X^2 least-squares fit, we can deduce the interval velocity (v_1) and thickness (d_1) of the first layer. To give a complete relationship between reflection time and offset for the case of more than one layer, TANER and KOEHLER (1969) related equations (1) and (2) through an infinite series of the following form

$$T^2(X) = C_0 + C_1X^2 + C_2X^4 + C_3X^6 + \cdots, \quad (7)$$

where C_i, ($i = 0, 1, 2, \ldots$) are functions of velocities and thicknesses of layers concerned. The first coefficient represents the square of the two-way travel time at zero offset and the second one is the inverse square of the rms velocity. Depending on the velocity variation, the series can be truncated to Dix's hyperbolic (two coefficients) approximation only at very small offset where refraction effects at all overlying interfaces are negligibly small. Large refractions take place at large offsets, and calculation of interval velocities from these travel times will be erroneous unless refraction effects are taken into account.

For a given velocity model and prescribed take-off angles at the source, travel times $T(X)$ at various offsets X covering the gamut of low-angle and wide-angle range reaching offsets say five times the depth of the bottom of the last layer of the model shown in Figure 3 can be calculated using equations (1) and (2). The exact ray parameters at various offsets are calculated using Snell's law by equation (3),

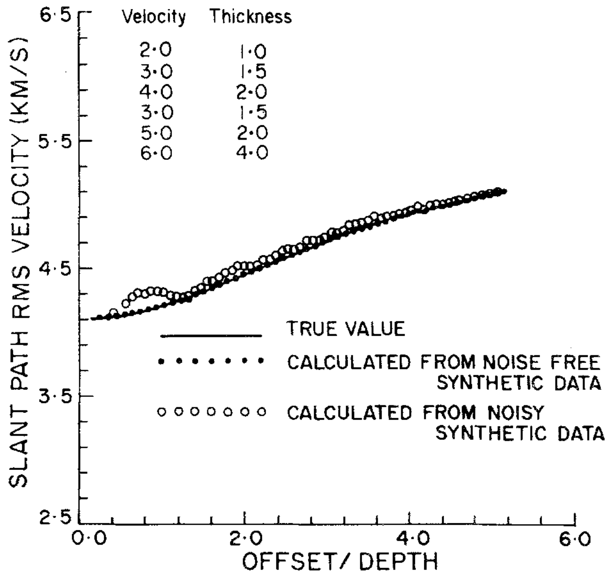

Figure 3
Comparison between true slant path rms velocity and the one calculated by the proposed method from noisy and noise-free synthetic reflection travel times for the model shown in the figure. Slant path rms velocity at the midpoint of each segment is shown.

corresponding to different prescribed take-off angles at the source, and have been plotted in Figure 2 against offset/depth ratio. The solid curve represents the true ray parameter. Now the question arises, is it possible to calculate ray parameters quite accurately at all points from a set of discrete travel-time data at increasing offset? Our answer to this question is yes, it is possible, and we have shown here how to calculate the ray parameters quite accurately by a new approach using wide-angle reflection times, even when contaminated by random errors. This method is described below.

The travel times calculated from the bottom most layer of the model displayed in Figure 3 are segmented such that each segment contains some points, say 15, in a manner that the first segment contains the first to fifteenth point, the second segment the second to sixteenth point, the third segment the third to seventeenth point and so on. The approximate rms velocity, obtained by hyperbolic least squares fit to the increasing offset travel times at various segments, is better termed as slant path rms velocity (ROBINSON, 1983), and the hyperbolic relation is written as

$$T^2(X) = X^2/V^2_{\mathrm{sprms}} + T^2_{\mathrm{sp}\,0}. \tag{8}$$

where $T_{\mathrm{sp}\,0}$ is the two-way travel time corresponding to the slant path rms velocity V_{sprms}. Considering V_{sprms} and $T_{\mathrm{sp}\,0}$ approximately constant over a reasonable length of a travel-time segment, we can differentiate equation (8) with respect to offset X as

$$T\,dT/dX = X/V_{\mathrm{sprms}}^2, \tag{9}$$

where dT/dX is nothing but the ray parameter (p). Each point of the set is associated with its individual slant path rms velocity and ray parameter, both of which increase with increasing offset. The actual V_{sprms} at different (X_i, T_i)-coordinates can be calculated by equation (9) using exact ray parameters as shown in Figure 2 by a solid line. The true V_{sprms} values are plotted against the offset/depth ratio in Figure 3 for the model shown in this figure itself. When noise-free synthetic data are used, segmenting all travel times containing only three points at a time produces the V_{sprms} indicated by dots in Figure 3, which falls quite accurately on the solid line curve. This has been plotted at the second point of each segment against its distance, divided by the depth of the bottom interface of the last layer from which reflection times have been calculated. Once we know V_{sprms} from travel times only, we can calculate the ray parameter using Equation (9) and the same shown by dots are plotted against offset/depth in Figure 2. We see that they also fall on the true curve, indicated by the solid line. When the data contain errors, the trend, as a whole, increases with increasing offset but the values differ in its close vicinity and the variations depend on the number of points taken into consideration for fitting. For noisy data we have to take as many data points in a segment as possible. From the contaminated data with errors lying between -50 ms and $+50$ ms for the model under consideration we see that many points, say more than twenty data points in one segment, produce a very good estimate of V_{sprms} shown in Figure 3 by open circles. These have been plotted at the midpoint of each segment, divided by the depth of the bottom interface of the last layer. Correspondingly, we can calculate the ray parameters from noisy travel-time data using Equation (9), and the same have been plotted against offset/depth in Figure 2 by open circles. This shows a very good estimation of the ray parameter. It is to be noted that the ray parameter, calculated by this method, is valid only at the midpoint of the segment. Also to be considered are the ray parameters at other points of the segment, which are calculated as follows.

The tangent drawn to a point of a theoretical reflection travel-time curve produces the ray parameter at that point for the reflected phase. For a set of discrete data, the ray parameter at a point can be calculated by the finite-difference method from data lying very closely on both sides of the point at equal interval. This is equivalent to drawing a straight line based on a least-square fit to the three travel-time data as

$$T = pX + C, \tag{10}$$

the slope (p) of which produces the ray parameter at the midpoint. To gain accurate value of the ray parameter, travel times should be very accurate and data

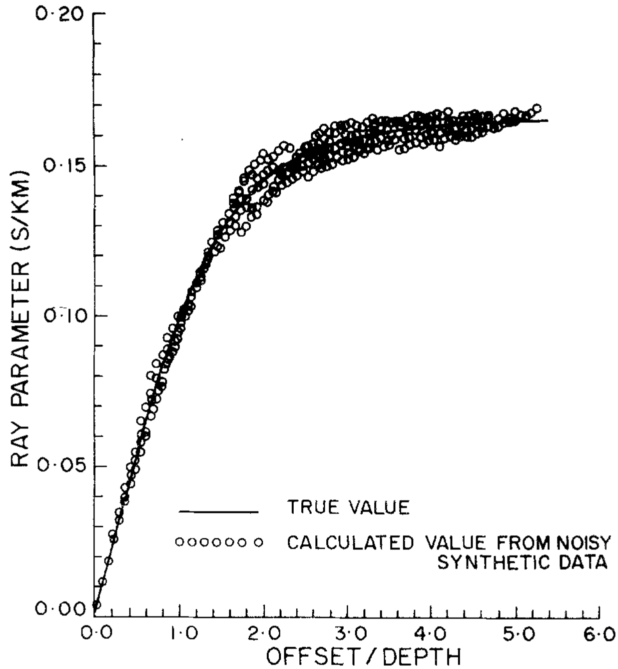

Figure 4

Comparison between true ray parameters and those calculated using equation (9) at all points of each travel time segment using noisy synthetic reflection travel times for the model indicated in Figure 3. Ray parameters at all points of each segment are compared.

(or geophone) interval should be very small. For noisy data we must take data as numerous (here 21 points) as possible. The ray parameter calculated by Equation (10) and the one obtained by Equation (9) using the slant path rms velocity (corresponding to the 21 data points), are very similar. Now using the same slant path rms velocity, which is strictly valid at the midpoint of the segment consisting of a set of data points, when we calculate the ray parameters at all other points of the segment using Equation (9), we gain the ray parameters very close to the true values at the low-angle range, as is evident from Figure 4. This figure also indicates that the calculated values of ray parameters display some variance from the true values at sufficiently large offset, i.e., in the wide-angle range (more than offset/depth ratio of 2.0). It is clearly observed from Figure 2 that the ray parameters at wide-angle range increase very slowly. We notice from Figure 3 that the slant path rms velocity also increases with successively increasing offset. Hence, the ray parameter calculated as per Equation (9) at a point in the first half of the segment is always less than its normal value, because to calculate it we are using a slightly higher slant path rms velocity which is actually determined at the midpoint of the

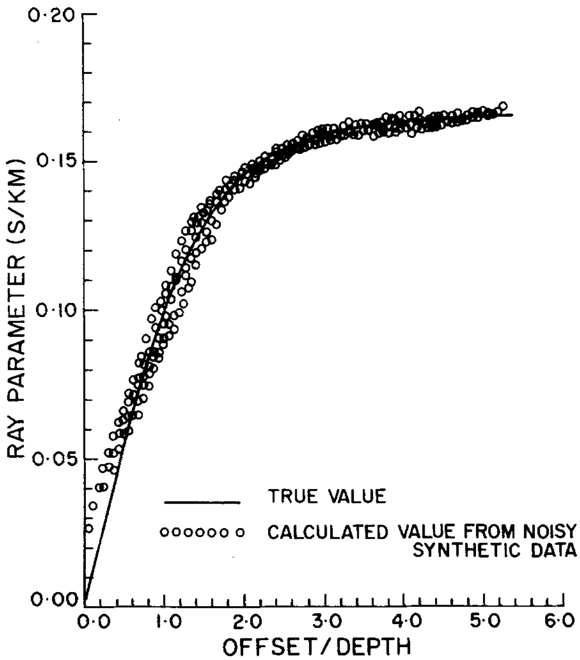

Figure 5
Comparison between true and calculated ray parameters, obtained by taking the average of the ray parameter calculated using Equation (9) and that with (10) from noisy synthetic reflection travel times for the model indicated in Figure 3. Ray parameters at all points of each segment are compared.

segment using Equation (8). On the other hand, the calculated ray parameters for points on the second half of the segment are always more than their true values due to the use of midpoint slant path rms velocity which is slightly smaller than that which should have been used for the points. By taking the average of the calculated dT/dX values determined as per Equation (9) at various points of the segment and the estimated dT/dX at the midpoint of the segment as obtained by Equation (10), quite accurate values of ray parameters are obtained. Figure 5 shows these ray parameters at different points calculated from various segments of increasing offset reflection travel times. To illustrate how well the principle works, we have taken twenty (X, T) data points in a segment as a specimen lying between 32.8 to 40.8 km offset distance at 400 m interval for the model shown in Figure 3. Corresponding to these twenty data points, true ray parameters are already known and have been denoted in Figure 6 by the solid line. Using the above principle, we calculate the ray parameters at different points of the segment from noise-free and noisy synthetic data. They are shown in the same figure by dots and open circles respectively for noise-free and noisy data. This clearly shows that there are slight differences between the true ray parameters and the calculated ones from both the noisy and

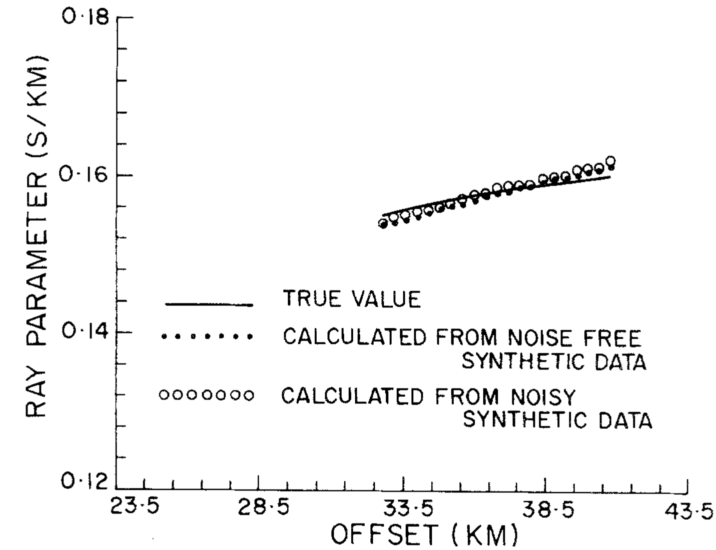

Figure 6
Comparison between true and calculated ray parameters in the distance range between 32.8 to 40.8 km by the present method from noisy and noise-free synthetic reflection travel times for the model described in Figure 3.

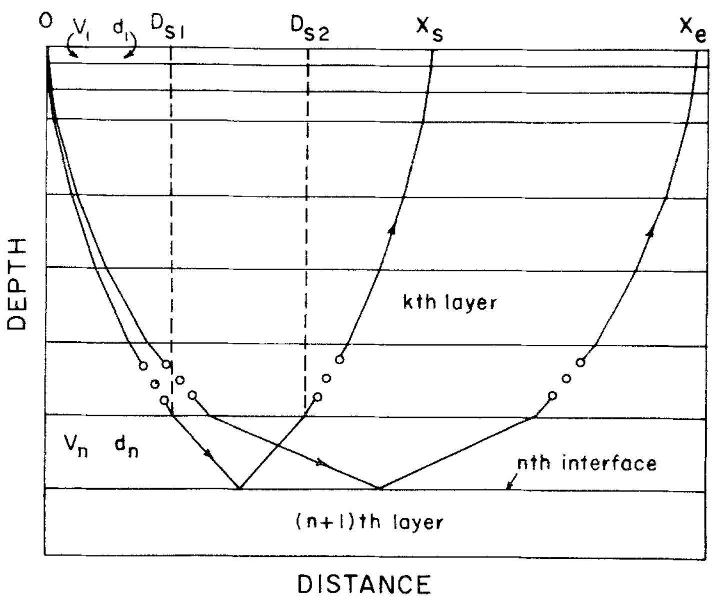

Figure 7
Reflection ray paths for two extreme ends of a recording spread lying between X_s and X_e km for a medium of homogeneous, isotropic, and horizontal layers with various parameters defined.

noise-free data by the proposed method. Please notice the scale for the ray parameters in Figure 6, which is highly exaggerated. It is observed from Figure 6 that ray parameters for points on the first half of the segment are slightly underestimated, whereas those for the second half are slightly overestimated.

Let us now see how we can strip off the contributions in the offsets and travel times associated with overlying layers. Referring to Figure 7, we are interested in calculating the interval velocity and layer thickness of the nth layer from wide-angle reflection times for which end values are T_s and T_e from the nth interface in the distance range between X_s and X_e with respect to the source at O. Of course, we assume that the layer parameters (velocities and thicknesses) of all overlying $(n-1)$ layers are known. Using the principle described in earlier paragraphs we can calculate the ray parameters at other offsets lying between X_s and X_e, with their values being p_s and p_e at the end points respectively. The offset contribution of all the overlying $(n-1)$ layers to the total offsets corresponding to the ray parameter p_s is given by

$$X_s(n-1) = OD_{s1} + D_{s2}X_s \tag{11}$$

$$= 2p_s \sum_{k=1}^{n-1} d_k v_k / [1 - p_s^2 v_k^2]^{1/2}. \tag{12}$$

The travel-time contribution by all $(n-1)$ layers corresponding to the ray parameter p_s is expressed as

$$T_s(n-1) = 2 \sum_{k=1}^{n-1} d_k / [v_k(1 - p_s^2 v_k^2)^{1/2}]. \tag{13}$$

The travel time associated with the nth layer for the ray parameter p_s is

$$T_{ns} = T_s - T_s(n-1), \tag{14}$$

where T_s is the travel time at offset X_s from the nth interface. The offset associated with the nth layer for the ray parameter p_s is

$$X_{ns} = X_s - X_s(n-1). \tag{15}$$

Similarly, the travel time and offset associated with the nth layer for the ray parameter p_e corresponding to the end point data (X_e, T_e) are given by the expression

$$T_{ne} = T_e - T_e(n-1), \tag{16}$$

$$X_{ne} = X_e - X_e(n-1), \tag{17}$$

where $T_e(n-1)$ and $X_e(n-1)$ are the contributions to travel time and offset corresponding to the end ray parameter p_e for all overlying $(n-1)$ layers. In this way, offsets and travel times for the nth layer, corresponding to all other ray parameters lying between p_s and p_e, can be calculated. These are related to the interval velocity v_n and thickness d_n of the nth layer through the hyperbolic equation

$$T_n^2 = X_n^2/v_n^2 + 4\,d_n^2/v_n^2. \tag{18}$$

Least-squares hyperbolic fitting to these points directly gives the interval velocity and thickness of the nth layer.

In reality, seismic velocity within a layer varies both laterally and vertically, and interfaces are often not horizontal. Hence, the assumption of a flat layered earth model and the errors in observed (X, T) data and those in calculating the ray parameters at the observation points will produce a mean error in the resulting velocity of the nth layer

$$m(v_n) = \left(\frac{v_n^3}{2}\right) m(T_n^2) \left[\frac{k}{k \sum_{i=1}^{k} X_{ni}^4 - \left(\sum_{i=1}^{k} X_{ni}^2\right)^2}\right]^{1/2}, \tag{19}$$

where $m(T_n^2)$ is the mean error of squared offset times for the nth layer and k is the total number of (X_n, T_n) pairs lying between X_s and X_e. The mean error in the resulting thickness of the nth layer is calculated as,

$$m(d_n) = \left(\frac{v_n^2}{8\,d_n}\right) m(T_n^2) \left[\frac{\sum_{i=1}^{k} X_{ni}^4}{k \sum_{i=1}^{k} X_{ni}^4 - \left(\sum_{i=1}^{k} X_{ni}^2\right)^2}\right]^{1/2}. \tag{20}$$

Synthetic and Field Examples

To show the efficacy of the method, it is always preferable to apply the technique on synthetic data contaminated by some random noise, where the model to be estimated is known. A simplified nine-layered velocity model of the continental type crust in the West Bengal basin, India, has been shown in Figure 8 by the solid line curve. Corresponding to various interfaces, wide-angle reflection times are analytically computed using the parametric Equation (1) at offsets defined by Equation (2) by providing various take-off angles at the source. The reflection times are then contaminated by random errors with a specified value of 50 ms to simulate a field situation. The specified value of 50 ms in the random number generator (PRESS *et al.*, 1986) adds errors randomly lying between -50 to $+50$ ms to the reflection times associated with different interfaces. These synthetic data limited to the wide-angle range are shown in Figures 9(a), (b), (c) and (d) for different phases. Figure 9(a) contains two sets of wide-angle synthetic data for the first two layers. Figure 9(b) exhibits data for the third, fourth and fifth layers. The synthetic data for the sixth and seventh layers are displayed in Figure 9(c).

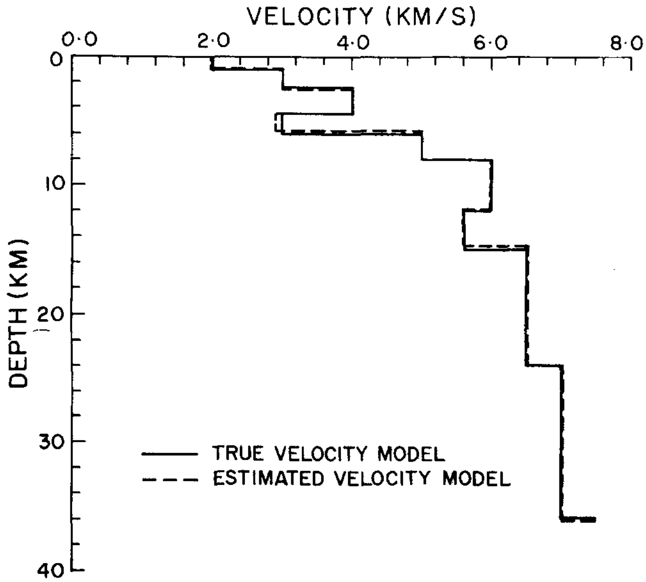

Figure 8
A nine-layered true velocity model, compared with the estimated velocity model obtained by the present method using wide-angle synthetic reflection travel times (shown in Figure 9).

Synthetic data for the eighth and ninth layers are shown in Figure 9(d). The data have been shown for clarity at every third data point in a reduced time scale with a reduction velocity of 6.0 km/s. Since reflection times for the first layer are purely hyperbolic, least-squares fit to the travel-time data with a hyperbolic equation directly gives the velocity and thickness of the first layer. Once estimated, the first layer parameters are held fixed for the estimation of the second layer parameter. Using the proposed method, we extract velocity information in a layer-by-layer fashion from all reflected phases. The estimated parameters are denoted in Figure 8 by the dashed line. This illustrates a very good agreement between the true model and the estimated model by the proposed method. The mean error in interval velocities and layer thicknesses, obtained from wide-angle reflection times by the proposed method, are calculated using Equations (19) and (20). They are shown in Table 1 against the estimated parameters. We see from Table 1 that mean errors in velocities and thicknesses do not follow any increasing trend with growing depth. This is because errors in velocity and thickness are random in nature and they may be affecting the computed offset and time contributions due to various layers in a random manner, not leading to any cumulative or systematic effects on the computation of layer parameters from one layer to the next. This indicates the reliability of the proposed method. To demonstrate how well the estimated model fit the data, we have computed the rms residual between the synthetic data and the travel times of the estimated model for different layers. This is also shown in Table

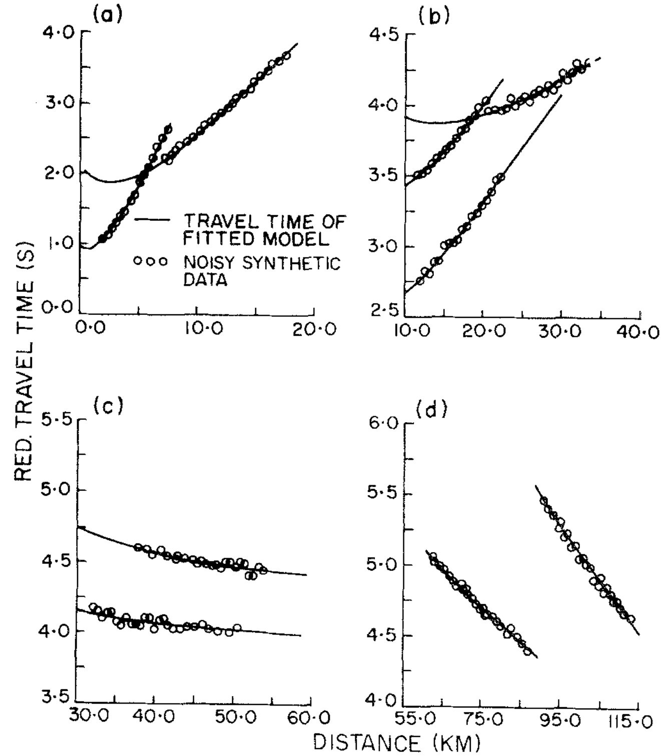

Figure 9
Synthetic reflection travel times from various interfaces of the true model shown in Figure 8, with random errors added and their comparison with the travel time curves generated for the estimated model. Time scale with reduction velocity of 6.0 km/s has been used in (a), (b), (c) and (d).

Table 1

Error analysis in interval velocity and layer thickness as determined from wide-angle seismic reflection travel times

Layer number	True velocity (km/s)	Estimated velocity (km/s)	True thickness (km)	Estimated thickness (km)	Travel time residual (rms) (s)
1	2.00	1.98 ± 0.02	1.00	0.96 ± 0.04	0.018
2	3.00	3.02 ± 0.02	1.50	1.68 ± 0.06	0.028
3	4.00	4.02 ± 0.03	2.00	1.83 ± 0.08	0.026
4	3.00	2.91 ± 0.06	1.50	1.40 ± 0.06	0.015
5	5.00	5.00 ± 0.05	2.00	2.17 ± 0.18	0.027
6	6.00	5.99 ± 0.06	4.00	3.85 ± 0.22	0.030
7	5.60	5.58 ± 0.08	3.00	2.93 ± 0.18	0.024
8	6.50	6.52 ± 0.05	9.00	9.28 ± 0.22	0.021
9	7.00	7.02 ± 0.05	12.00	12.09 ± 0.43	0.030

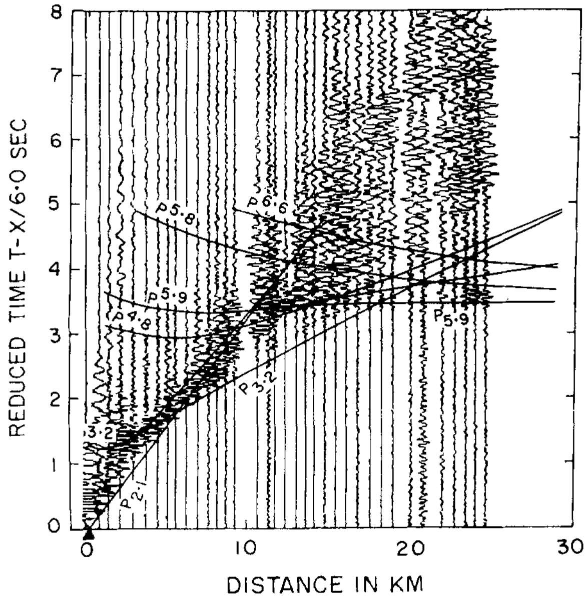

Figure 10

Field seismogram corresponding to shot point 25 along the Sadra–Degam part of the North Cambay DSS profile, India, (KAILA *et al.*, 1990) showing two subbasement reflections $P^{5.8}$ and $P^{6.6}$, travel times for which were used for the computation of an interval velocity model in Figure 11.

1 against the layer number. For all reflected phases we see that the rms residual is less than 0.03 s which indicates a first-rate match between the synthetic data and the calculated travel times of the estimated model. The travel times of the estimated model are shown in Figures 9(a)–(d) by solid lines.

We now use two field data sets to demonstrate the practical feasibility of the proposed method. For the assumption of the flat layered velocity model, the present technique gives averaged interval velocities and thicknesses of various layers. In deep seismic sounding investigations, usually the structure extending to the basement is interpreted using the refraction data, whereas the subbasement velocity structure upto the Moho is interpreted using strongly observable wide-angle reflection data by the 2-*D* forward modeling technique which is very time consuming and laborious.

Two well identified wide-angle reflected phases marked by $p^{5.8}$ and $p^{6.6}$ in Figure 10 from layers below the basement, corresponding to the shot point 25 along the Sadra–Mehmadabad–Degam part of a long profile in the North Cambay and Sanchor basins, India (KAILA *et al.*, 1990), have been used to find the velocity structure by the proposed method. Since we work layer-by-layer downward, we need velocity information at the shallow level up to the basement. The first arrival refraction data at the shallow level can be analyzed by one of many available refraction methods. As the 2-*D* velocity model in this region (KAILA *et al.*, 1990)

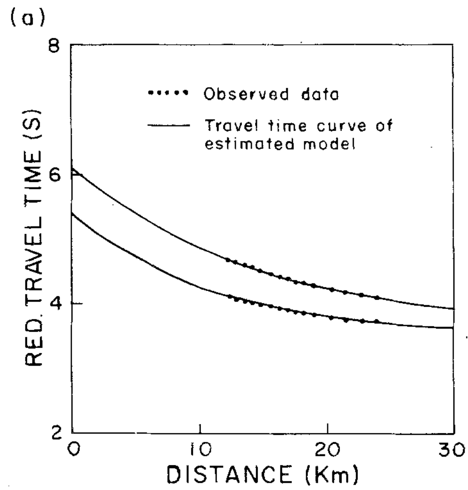

Figure 11(a)
Two wide-angle reflection data sets (reduction velocity = 6.0 km/s) recorded along the Sadra–Degam part of the North Cambay DSS profile, India (KAILA *et al.*, 1990), with the travel time curves generated for the estimated model given in 11(b) as determined by the present method.

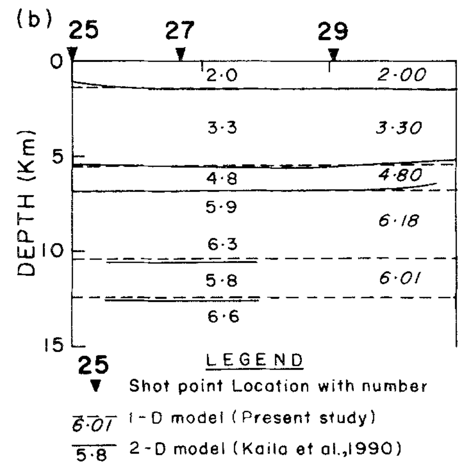

Figure 11(b)
1-*D* velocity model, superimposed on a 2-*D* velocity model available along the above profile.

is more or less flat, we have averaged out the velocity values in the first three layers (obtained by forward refraction modeling) to a simplified three layer $1-D$ interval velocity model, indicated by velocity values in italics and thicknesses by dashed lines in Figure 11(b). The first layer with a velocity of 2.00 km/s and a thickness of 1.32 km, the second layer with a velocity of 3.30 km/s and a thickness of 4.00 km, and the third layer with a velocity of 4.80 km/s and a thickness of 1.55 km are held fixed while dealing with the two subbasement wide-angle reflection travel-time ranges shown in Figure 11(a) by dots. Here also, data are plotted in a reduced time scale with a reduction velocity of 6.0 km/s at every third data point. The first reflected phase gives the interval velocity of 6.18 ± 0.04 km/s and the thickness of 3.67 ± 0.05 km with rms residual of 0.013 s. The second reflected phase gives interval velocity of 6.01 ± 0.03 km/s and thickness of 2.11 ± 0.03 km with rms residual of 0.014 s. The estimated layer parameters are shown by velocity values written in italics at the right-hand side of Figure 11(b) and the thickness or depth by dashed lines. The theoretical reflection times corresponding to the estimated velocity model are designated by solid lines in Figure 11(a). As the present method is based on the exact ray theory and the calculation of ray parameters is quite accurate, there is no problem with the estimation of the low velocity zone (LVZ) in the upper crust.

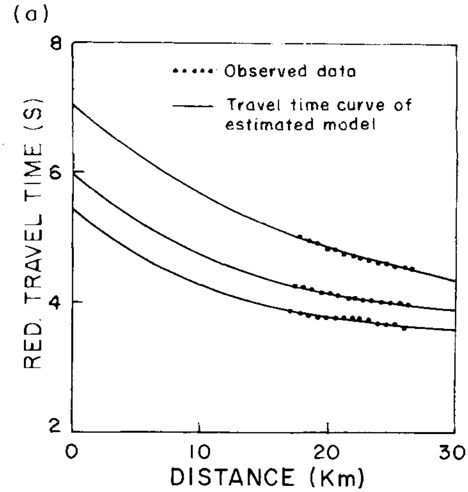

Figure 12(a)
Three wide-angle reflection data sets recorded along the Burdwan–Satgachia–Dhatrigram part of the Beliator–Burdwan–Bongaon DSS profile in the West Bengal basin, India (KAILA *et al.*, 1992), with the travel time curves for the estimated model given in (b), as determined by the present method.

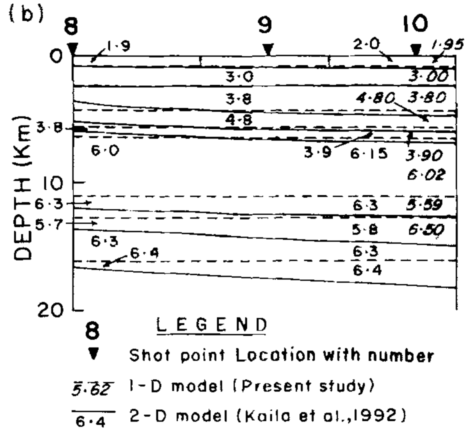

Figure 12(b)
1-*D* velocity model, superimposed on 2-*D* velocity structure along the above profile.

Another field example is given in Figure 12. Travel times of three wide-angle reflections are shown in Figure 12(a) by dots at every third data point, corresponding to the shot point 8 along the Beliator—Burdwan—Bongaon DSS Profile in the West Bengal basin, India (KAILA *et al.*, 1992). These reflections have been used to find the 1-*D* interval velocity structure of the crust in the Burdwan-Satgachia-Dhatrigram part. The 2-*D* velocity model (KAILA *et al.*, 1992) in this region is more or less flat. We have averaged out the first five layers up to the basement into a simplified five layered 1-*D* interval velocity model, indicated by velocity values in italics and thicknesses by dashed lines in Figure 12(b). The velocities of the first five layers are 1.95, 3.00, 3.80, 4.80 and 3.90 km/s, respectively. The corresponding thicknesses are 0.95, 1.55, 2.10, 1.10 and 1.00 km, respectively. These layer parameters are held fixed as is conventionally done in a layer-by-layer processing work for the investigation of the deeper crustal structure in terms of interval velocities and layer thicknesses. By the method proposed above we receive the interval velocity of 6.02 ± 0.07 km/s and thickness of 4.49 ± 0.10 km from the first wide-angle reflected phase with rms residual of 0.02 s. The second reflected phase gives the interval velocity of 5.59 ± 0.06 km/s and thickness of 1.76 ± 0.09 km with rms residual of 0.018 s. The third reflected phase gives an interval velocity of 6.50 ± 0.09 km/s and a thickness of 3.35 ± 0.12 km with rms residual of 0.021 s. The estimated layer parameters are indicated by velocity values written in italics at the right-hand side of Figure 12(b) and the thickness or depth by dashed lines. Here also we see that a low velocity zone (5.59 km/s) is present in the upper crust just below the basement layer of velocity 6.02 km/s. The velocity of the LVZ is a little less than the one obtained by 2-*D* forward modeling. Since we have assumed a flat layered earth model, the effect of the lateral variation of velocity in all overlying layers plays a role in determining the layer parameters of deeper layers. As a consequence, we derive the averaged interval velocity of the sixth layer as 6.02 km/s. This layer extends to a depth of 11.19 km. The 2-*D* reflector depth for this layer in the region varies between 12.0 to 13.0 km from shot point 8 towards shot point 10. The estimated thickness of LVZ (5.59 km/s) is only 1.76 km, whereas that for 2-*D* modeling varies between 1.90 to 2.30 km from shot point 8 towards shot point 10. The bottom interface of the present model, obtained by the proposed method, has risen to a depth of 16.30 km, whereas the 2-*D* depth range lies between 16.65 km below shot point 8 and 18 km below shot point 10. As a whole, the estimated 1-*D* velocity model by the present method matches quite well with the available 2-*D* velocity model (KAILA *et al.*, 1992).

Conclusions

The layer stripping method proposed here estimates the layer parameters, i.e., interval velocities and thicknesses, quite accurately as it is based on the exact ray theory. The method is mathematically very simple and can be easily adopted for the velocity estimation from any wide-angle reflection times. Being very fast, the method helps to process a large volume of wide-angle seismic reflection data in a deep seismic sounding investigation to engender an approximate 1-*D* crustal velocity structure within a very short time. The assumption of a flat layered earth model and errors in observed (X, T) data and those in calculated ray parameters produce mean errors in the estimated layer parameters but they do not propagate downward systematically from one layer to the next, making the proposed method very reliable. If the associated errors are estimated substantial, the present method indicates a need to refine the velocity structure further by 2-*D* modeling. The 1-*D* models, independently obtained from different sets of reflection times from various shot points along a profile, when plotted together in their respective distance-depth location, will produce a pseudo 2-*D* velocity picture of the subsurface. This will serve as a superior initial model to either 2-*D* forward modeling or 2-*D* inversion modeling.

Acknowledgements

The authors are grateful to Dr. Harsh K. Gupta, Director, NGRI for his constant encouragement to carry out this work and permission to publish the same.

The first author (K. Sain) wishes to thank the Council of Scientific and Industrial Research, India, for providing him with a research fellowship. Finally, the authors would like to thank Dr. S. Treitel and two anonymous reviewers for their excellent suggestions to improve the quality of the paper.

References

AL-CHALABI, M. (1974), *An Analysis of Stacking, Average and Interval Velocities of a Horizontally Layered Ground*, Geophys. Prosp. *22*, 458–475.

BESSONOVA, E. N., FISHMAN, V. M., RYABOYI, V. Z., and SITNIKOVA, G. A. (1974), *The Tau Method for Inversion of Travel Times, I. Deep Seismic Sounding Data*, Geophys. J. Roy. Astr. Soc. *36*, 377–398.

BROWN, R. J. S. (1969), *Normal Moveout and Velocity Relations for Flat and Dipping Beds and for Long Offsets*, Geophys. *34*, 180–195.

BULLEN, K. E., and BOLT, B. A., *An Introduction to the Theory of Seismology* (Cambridge University Press, Cambridge, U.K. 1985).

CRESSMAN, K. S. (1968), *How Velocity Layering and Steep Dip Affect CDP*, Geophys. *33*, 399–411.

CUTLER, R. T., and LOVE, P. L. (1980), *Elliptical Velocity Analysis* (abstr.), Geophys. *45*, 540.

DIEBOLD, J. B., and STOFFA, P. L. (1981), *The Travel Time Equation $\tau - p$ Mapping and Inversion of Common Midpoint Data*, Geophys. *46*, 238–254.

DIX, C. H. (1955), *Seismic Velocities from Surface Measurements*, Geophys. *20*, 68–86.

FUCHS, K., and MUELLER, G. (1971), *Computation of Synthetic Seismograms with the Reflectivity Method and Comparison with Observations*, Geophys. J. Roy. Astr. Soc. *23*, 417–433.

GARMANY, J., ORCUTT, J., and PARKER, R. (1979), *Travel Time Inversion: A Geometrical Approach*, J. Geophys. Res. *84*, 3615–3622.

GIESE, P., STEIN, A., and PRODEHL, C., *Explosion Seismology in Central Europe—Data and Results* (Berlin-Heidelberg-New York, Springer-Verlag 1976).

HUBRAL, P., and KREY, T., *Interval Velocities from Seismic Reflection Time Measurements* (The Society of Exploration Geophysicists Monograph, Tulsa 1980).

KAILA, K. L., and KRISHNA, V. G. (1979), *A New Computerized Method for Finding Effective Velocity from Reversed Reflection Travel Time Data*, Geophys. *44*, 1064–1076.

KAILA, K. L., REDDY, P. R., MALL, D. M., VENKATESWARLU, N., KRISHNA, V. G., and PRASAD, A.S.S.S.R.S. (1992), *Crustal Structure of the West Bengal Basin, India, from Deep Seismic Sounding Investigations*, Geophys. J. Internat. *111*, 45–66.

KAILA, K. L., and SAIN, K. (1994), *Errors in rms Velocity and Zero Offset Two-way Time as Determined from Wide-angle Seismic Reflection Travel Times Using Truncated Series*, J. Seis. Explor. *3*, 173–188.

KAILA, K. L., TEWARI, H. C., KRISHNA, V. G., DIXIT, M. M., SARKAR, D., and REDDY, M. S. (1990), *Deep Seismic Sounding Studies in the North Cambay and Sanchor Basins, India*, Geophys. J. Internat. *103*, 621–637.

LIMOND, W. Q., and PATRIAT, Ph. (1975), *The Accuracy of Determination of Seismic Velocities from Variable Angle Reflection (Disposable Sonobuoy) Records*, Geophys. J. Roy. Astr. Soc. *43*, 905–938.

NOWROOZI, A. A. (1990), *Interpretation of Seismic Reflection Records: Direct Calculation of Interval Velocities and Layer Thicknesses from Travel Times*, Pure Appl. Geophys. *133*, 103–115.

PRESS, W. H., FLANNERY, B. P., TEUKOLSKY, S. A., and VETTERLING, W. T., *Numerical Recipes: The Art of Scientific Computing* (Cambridge University Press, Cambridge, U.K. 1986).

RICHARDS, T. C. (1961), *Motion of the Ground on Arrival of Reflected Longitudinal and Transverse Waves at Wide-angle Reflection Distance*, Geophys. *26*, 277–297.

ROBINSON, E. A., *Seismic Velocity Analysis and the Convolution Model* (D. Reidel Publishing Co., Dordrecht/Boston/Lancaster 1983).

SAIN, K., and KAILA, K. L. (1994), *Inversion of Wide-angle Seismic Reflection Times with Damped Least Squares*, Geophys. *59*, 1735–1744.

SATTLEGGER, J. (1965), *A Method of Computing Interval Velocities from Expanding Spread Data in the Case of Arbitrarily Long Spreads and Arbitrarily Dipping Interfaces*, Geophys. Prosp. *13*, 306–318.

SCHULTZ, P. S. (1982), *A Method of Direct Estimation of Interval Velocities*, Geophys. *47*, 1657–1671.

STOFFA, P. L., and BUHL, P. (1980), *Two Ship Multichannel Seismic Experiments for Deep Crustal Studies*, J. Geophys. Res. *84*, 7645–7660.

STOFFA, P. L., BUHL, P., DIEBOLD, J. B., and WENGEL, F. (1981), *Direct Mapping of Seismic Data to the Domain of Intercept Time and Ray Parameter: A Plane Wave Decomposition*, Geophys. *46*, 255–267.

STOFFA, P. L., DIEBOLD, J. B., and BUHL, P. (1928), *Velocity Analysis for Wide Aperture Seismic Data*, Geophys. Prosp. *30*, 25–57.

TANER, M. T., COOK, B. B., and NEIDELL, N. S. (1970), *Limitations of the Reflection Seismic Method: Lessons from Computer Simulations*, Geophys. *35*, 551–573.

TANER, M. T., and KOEHLER, F. (1969), *Velocity Spectra Digital Computer Derivation and Application of Velocity Functions*, Geophys. *34*, 859–881.

WINTERSTEIN, D. F., and HANTEN, J. B. (1985), *Supercritical Reflections Observed in P- and S-wave Data*, Geophys. *50*, 185–195.

(Received November 7, 1994, accepted June 21, 1995)